

Effect of intermolecular interactions on charge and exciplex formation in high-performance organic semiconductors

Whitney E.B. Shepherd,^a Andrew D. Platt,^a Garrett Banton,^a David Hofer,^a
Marsha A. Loth,^b John E. Anthony^b and Oksana Ostroverkhova^a

^aDepartment of Physics, Oregon State University, Corvallis, OR 97331, USA;

^bDepartment of Chemistry, University of Kentucky, Lexington, KY 40506, USA

ABSTRACT

We present optical, photoluminescent (PL), and photoconductive properties of functionalized anthradithiophene (ADT) derivatives and their composites. Solution-deposited ADT films exhibit charge carrier mobilities of over $1.5 \text{ cm}^2/(\text{Vs})$, high PL quantum yields, and high photoconductivity. We show that molecular arrangement and intermolecular interactions significantly contribute to (opto)electronic properties of guest-host thin films of these pi-stacked materials. Specifically, the formation of aggregates plays an important role in establishing efficient conduction pathways in ADT derivatives dispersed in a host matrix. In addition, the extent and nature of aggregation and the resulting changes in PL and photoconductive behavior can be effectively manipulated through different film fabrications techniques. Furthermore, energy transfer and exciplex formation has been shown to occur between two different ADT derivatives, which also alters the photoconductive response of the systems. We explore the dependence of the photoconductive response of such guest-host systems on excitation wavelength.

Keywords: Organic Semiconductors, Photoconductivity, Aggregation, Exciplex

1. INTRODUCTION

Organic opto(electronic) materials are a promising class of materials due to their low-cost, tunable properties and potential applications ranging from display technologies to photovoltaics.^{1,2} A solution-processable functionalized, fluorinated anthradithiophene (ADT) derivative (ADT-TES-F) has been synthesized which exhibits charge carrier (hole) mobilities of over $1.5 \text{ cm}^2/\text{Vs}$ in spin-coated thin films,³⁻⁵ fast charge carrier photogeneration, and high continuous wave (cw) photoconductivity.^{6,7} Photoluminescent (PL) and photoconductive properties of this derivative have been shown to depend on the degree of aggregation present in various thin film composite systems.⁸ Furthermore, a combination of two ADT derivatives, ADT-TIPS-CN and ADT-TES-F, have been shown to exhibit strong energy transfer and exciplex formation in solid-state, leading to considerably different charge carrier dynamics at nanosecond time scales in thin films of this composite, as compared to those in pristine films.⁹⁻¹¹

In this paper, we explore variations in aggregate and exciplex formation depending on film preparation technique, and their effect on PL and photoconductive behavior. Furthermore, we explore the charge carrier dynamics in the ADT-TES-F/ADT-TIPS-CN composite system on a longer time scale of tens of seconds, and variation in the photoconductive response as a function of excitation wavelength.

2. EXPERIMENTAL

2.1 Materials and Sample Preparation

We studied thin films of two ADT derivatives, ADT-TES-F and ADT-TIPS-CN whose structures are shown in Figure 1. Synthesis and characterization of optical and electronic properties of ADT-TES-F and ADT-TIPS-CN have been reported elsewhere.^{4,6} The highest occupied and lowest unoccupied molecular orbital (HOMO and

Further author information: (Send correspondence to O.O.)

O.O.: E-mail: oksana@science.oregonstate.edu, Telephone: 1 541 737 1679

J.E.A.: E-mail: anthony@uky.edu, Telephone: 1 859 257 8844

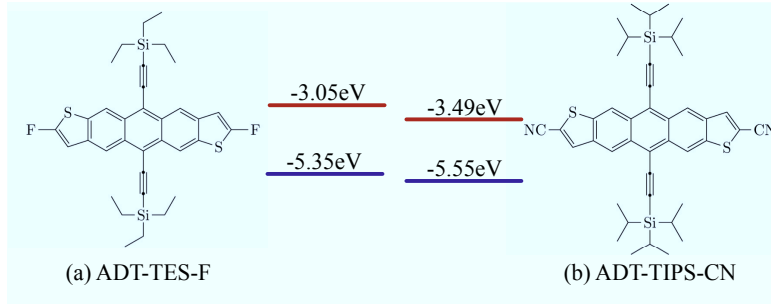


Figure 1. Molecular structures of (a) ADT-TES-F and (b) ADT-TIPS-CN. HOMO and LUMO levels of each material in solution are also shown.

LUMO, respectively) levels of ADT-TES-F and ADT-TIPS-CN were measured in solution using differential pulse voltammetry and are shown in Fig. 1.⁶

Pristine samples of ADT-TES-F for PL measurements were prepared via drop and spin casting. Spin cast samples were prepared from a stock solution of 3×10^{-2} M in toluene. Several drops were deposited on a glass substrate and allowed to dry partially before spinning at 4000 rpm for 50 s. Drop cast samples were prepared by placing a few drops of stock solution onto a glass substrate at $\sim 60^\circ\text{C}$.

Samples of ADT-TES-F in poly(methyl methacrylate) (PMMA) (75,000 M.W. from Polysciences, Inc.) for PL measurements were also prepared with an average spacing of 1 nm between adjacent ADT-TES-F molecules. The average spacing, ρ , between adjacent ADT-TES-F was determined according to $\rho = M/(N_A \rho_m f)^{1/3}$ where N_A is Avogadro's number, ρ_m is the mass density of the host and f is the molar fraction of guest to host.^{12,13} Stock solution of 10^{-5} M ADT-TES-F in toluene was added to 10^{-3} M stock solution of PMMA in toluene. The resulting mixture was either drop cast onto a clean glass substrate at $\sim 60^\circ\text{C}$, or spun onto a clean glass substrate at 600 rpm for 50 s. The drop cast sample is denoted P_1^{drop} and the spin cast sample is denoted P_1^{spin} .

Composite samples of ADT-TIPS-CN in ADT-TES-F for PL measurements were prepared from stock solutions in toluene of 3×10^{-2} M and 10^{-5} M, respectively. Spun and drop cast samples were prepared in the same manner as the pristine ADT-TES-F samples described above. The final concentrations in the films were 3.6×10^{-4} and 3.6×10^{-2} mols of ADT-TIPS-CN/liter of ADT-TES-F (M). Spin cast samples are denoted S(3.6×10^{-4} M) and S(3.6×10^{-2} M), and drop cast samples are denoted Dr(3.6×10^{-4} M) and Dr(3.6×10^{-2} M).

The optical density (OD) at the absorption maximum in all spin cast films did not exceed 0.25, which suggests film thicknesses of below $\sim 0.5 \mu\text{m}$.^{8,14} Drop cast films were thicker (e.g. 0.5-2 μm in the case of pristine ADT-TES-F films).⁷ The OD at the absorption maximum of the P_1^{drop} sample was ~ 2.8 .

For photoconductivity measurements, samples were prepared in the same manner as described above, except instead of clean glass substrates, the solutions were deposited onto glass substrates with photolithographically deposited 5 nm/50 nm thick Cr/Au interdigitated electrode pairs. Electrodes consisted of 10 pairs of 1 mm long fingers with 25 μm finger width and 25 μm gaps between the fingers of opposite electrodes.

2.2 Optical Properties

PL measurements of pristine ADT-TES-F films and ADT-TES-F in PMMA were taken at room temperature in a custom bulk fluorescence set up. 400 nm (frequency doubled Ti:Sapphire), 355 nm (cavity Q-switched Nd:YAG, 44.6 kHz rep rate from Nanolase) or 532 nm (frequency doubled Nd:YVO₄, Coherent, Inc.) laser light was used as the excitation source. No difference in PL emission spectra was seen under different illumination wavelengths. Emission was collected using a parabolic mirror and sent to a fiber coupled spectrometer (Ocean Optics USB2000) calibrated against a 3100 K black-body emitter.

PL measurements of composite ADT-TES-F/ADT-TIPS-CN samples were taken under 355 nm excitation. PL was collected via direct fiber pick-up and sent to the spectrometer described above.

2.3 Dark Current and Dc Photocurrent Measurements

For photoconductivity measurements, samples were placed in custom built fixtures and were illuminated from the substrate side. Either the 532 nm source described above or 633 nm excitation from a HeNe laser were used. A Keithley-237 source measure unit was used to apply voltage and measure current through the sample both in the dark and under illumination. The photocurrent was calculated as the difference between the two.

2.4 Spectral Fitting

Spectral fitting was performed using the multipeak fitting package in Igor Pro, which is an implementation of the Levenberg-Marquardt algorithm. Data was fit using a vertical offset and a series of gaussian functions.

3. RESULTS AND DISCUSSION

3.1 PL Properties

Morphology Variation in Pristine Thin Films Figure 2 shows PL spectra of pristine ADT-TES-F films fabricated via drop casting (a) and spin coating (b). Both films exhibited spectral features such as a red-shift and broadening of the spectra, as compared to those of ADT-TES-F in solution, due to exciton delocalization and intermolecular interaction.^{6,14} Also, PL spectra of both films exhibited vibronic progressions due to exciton-phonon coupling. The $0 \rightarrow 0$ peak in the spin cast sample occurs at ~ 585 nm and has been attributed to an ADT-TES-F aggregate.⁸ The ~ 625 nm and 692 nm peaks, also observed in the PL spectrum of this sample, are most likely due to coupling to vibrational modes. The spectrum of the drop cast film, which has not been corrected for self-absorption, has similar features: a ~ 603 nm peak (which would be much closer to a 585 nm peak, observed in the spin cast film, if accounted for self-absorption) and ~ 629 nm and 699 nm peaks due to coupling to vibrational modes. A slight red-shift of the latter as compared to similar peaks in the spectrum of the spin cast film are due to differences in film morphology, which changes local environment.⁸ In the drop cast film, however, the multipeak fitting identified additional spectral features at ~ 654 nm and 739 nm, which could be due to contributions from a different kind of an ADT-TES-F aggregate, not observed in thin spin cast films. Based on the PL spectral red-shift, it is possible that this aggregate has a larger size as compared to the aggregate characterized by a 585 nm dominant peak, which would increase exciton delocalization.

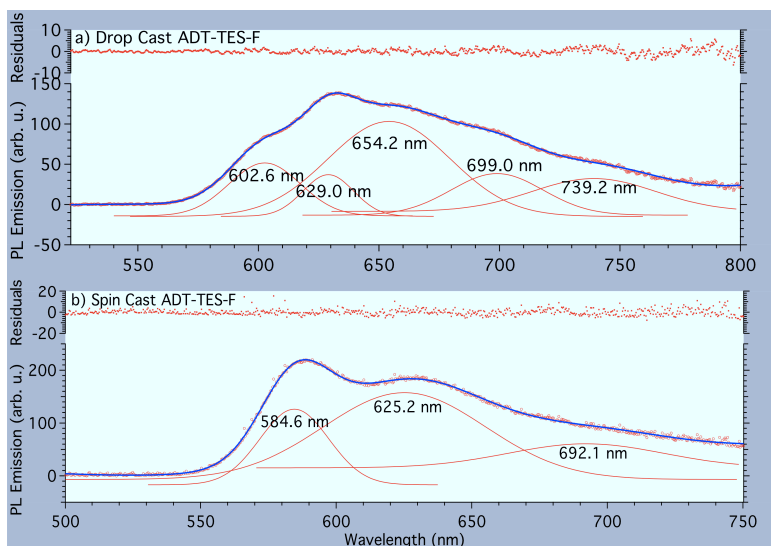


Figure 2. PL spectra of (a) drop and (b) spin cast ADT-TES-F films. Multipeak fitting shows variation in PL signature between films made by different deposition techniques.

Aggregation Effects in Different Host Matrices PL spectra of ADT-TES-F added to different host matrices of spin and drop cast PMMA are shown in Fig. 3. In P_1^{spin} , the spectrum consists of additive contributions from isolated ADT-TES-F molecules and ADT-TES-F aggregates.⁸ In P_1^{drop} there is no quantifiable contribution from isolated ADT-TES-F to the emission spectrum, in part due to self-absorption effects.

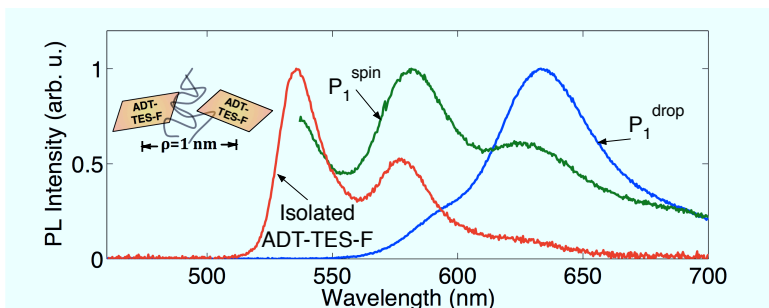


Figure 3. PL from a spin cast (P_1^{spin}) and drop cast (P_1^{drop}) PMMA film with ADT-TES-F embedded in it at an average spacing of 1 nm. P_1^{spin} spectrum has been corrected for self absorption, P_1^{drop} has not. Spectrum of isolated ADT-TES-F molecules is also plotted for reference.

PL spectrum of P_1^{spin} exhibits peaks at ~ 585 nm and 625 nm, which are attributed to the ADT-TES-F aggregate similar to that in a spin cast film of pristine ADT-TES-F (Fig. 2b).⁸ Spectrum of the P_1^{drop} sample has a peak at 593 nm (which is likely the same peak as the 585 nm peak seen in P_1^{spin}) whose contribution to an overall spectrum is greatly reduced due to self absorption. Also present in the spectrum of the P_1^{drop} sample are the peaks at ~ 625 nm (due to an ADT-TES-F aggregate identified in both spin cast and drop cast films in Fig. 2) and at ~ 650 nm (due to a larger ADT-TES-F aggregate which is only present in the drop cast ADT-TES-F pristine film in Fig. 2a). This suggests that in the ADT-TES-F/PMMA films, as in the ADT-TES-F pristine films, aggregation proceeds differently in the drop cast film, P_1^{drop} , as compared to that in the spin cast film, P_1^{spin} . As we show below, this results in dramatically different photoconductive properties of P_1^{drop} and P_1^{spin} samples.

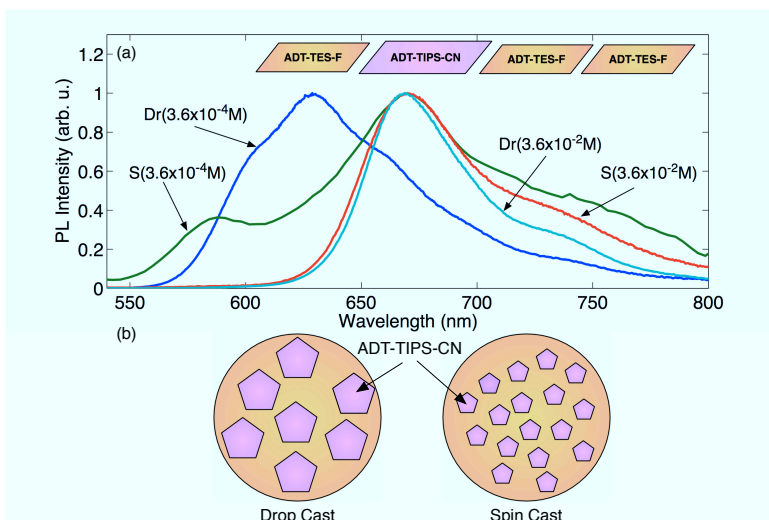


Figure 4. (a) PL from spin cast ADT-TES-F/ADT-TIPS-CN composite samples at two different concentrations, $S(3.6 \times 10^{-4}M)$ and $S(3.6 \times 10^{-2}M)$, and drop cast composite samples at the same concentrations, $Dr(3.6 \times 10^{-4}M)$ and $Dr(3.6 \times 10^{-2}M)$. (b) Schematic showing different size aggregates formed in drop and spin casted ADT-TES-F films. In the spin cast film the area of interaction between donor and acceptor is much higher than that in the drop cast film.

Energy Transfer and Exciplex Formation Between Two ADT Derivatives Energy transfer has been shown to occur between two ADT derivatives, ADT-TES-F and ADT-TIPS-CN.¹⁰ Furthermore, an exciplex can form between ADT-TES-F which acts as an electron donor and ADT-TIPS-CN which acts as an electron acceptor.¹¹ Composite films of ADT-TIPS-CN guest molecules embedded in a host of ADT-TES-F exhibit different behaviors in different film morphologies. Figure 4a shows spectra from two spin (S) and two drop (Dr) cast samples at two different concentrations of ADT-TIPS-CN in ADT-TES-F, 3.6×10^{-4} M and 3.6×10^{-2} M.

In S(3.6×10^{-4} M), S(3.6×10^{-2} M), and Dr(3.6×10^{-2} M), a ~ 668 nm peak dominates the spectra. This peak represents a photon energy of 1.86 eV which corresponds to the energy gap between the HOMO level of the donor (ADT-TES-F) and the LUMO level of the acceptor (ADT-TIPS-CN), and results from the decay of an exciplex formed across these two states.¹¹ The ~ 668 nm peak accounts for 68% of the total emission in S(3.6×10^{-4} M), 55% in S(3.6×10^{-2} M), and 47% in Dr(3.6×10^{-2} M). Percentages were determined from the area under the ~ 668 nm peak as found from fitting of the spectra in a similar manner to those shown in Fig. 2. In the Dr(3.6×10^{-4} M) sample, the multipeak fitting did not identify significant contributions of the exciplex emission at ~ 668 nm to the overall spectrum, as the PL spectrum in this sample was similar to that measured in a drop cast pristine ADT-TES-F film (Fig. 2a). Thus, at both ADT-TIPS-CN concentrations, the percentage of the emission due to the exciplex was higher in the spin cast film than the drop cast one. This is consistent with the formation of larger aggregates in drop cast films over spin cast films. Indeed, larger areas of aggregation reduce the available surface area for interaction between donor and acceptor as schematically shown in Fig. 4b.

3.2 Photoconductive Properties

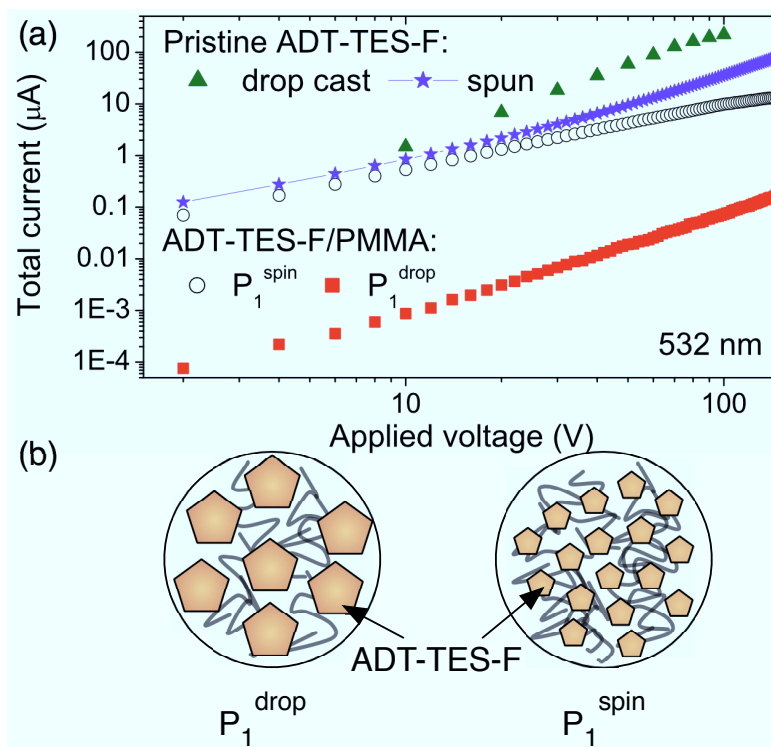


Figure 5. (a) Current under 532 nm cw excitation in drop and spin cast pristine ADT-TES-F films, as well as of P_1^{drop} and P_1^{spin} . Data on P_1^{drop} , P_1^{spin} and the spin cast pristine sample were taken at 15 mW/cm^2 , and data on the drop cast pristine sample was taken at 0.58 mW/cm^2 . (b) Schematic illustrating different aggregation properties in spin and drop cast ADT-TES-F/PMMA films. Based on the data in (a), the average distance between adjacent aggregates is likely to be considerably higher in the P_1^{drop} sample, as compared to that in P_1^{spin} .

ADT-TES-F Films Current under cw 532 nm illumination measured in spin and drop cast pristine ADT-TES-F and ADT-TES-F/PMMA films is shown in Figure 5a. In the case of the pristine films, the drop cast

film was considerably thicker; additionally, it contained larger aggregates conducive to charge carrier transport,⁸ which lead to a higher current amplitude. In the case of the ADT-TES-F/PMMA films, the opposite effect was observed. Although the drop cast film P_1^{drop} was similarly thicker than the spun cast film P_1^{spin} , which would be expected to produce a higher photocurrent, a considerably lower current amplitude was observed in the drop cast film P_1^{drop} . This could be due to the presence of large aggregates in the P_1^{drop} film, identified in the PL spectrum (Fig. 3), which are absent in the P_1^{spin} film. Indeed, at same ADT-TES-F concentrations in the drop and spin cast ADT-TES-F/PMMA films, larger aggregates in the P_1^{drop} film would mean larger average spacing between aggregates in this sample (Fig. 5b). Since PMMA provides a large energy barrier for charge transport, the larger distance would inhibit charge transport between aggregates in P_1^{drop} ,¹⁵ resulting in currents several orders of magnitude lower in this film as compared to those in P_1^{spin} .

ADT-TES-F/ADT-TIPS-CN Composite Films Figure 6 shows cw photocurrent obtained in $S(3.6 \times 10^{-2}M)$ under 15 mW/cm^2 532 nm and 633 nm excitation. 633 nm light primarily excited the acceptor (ADT-TIPS-CN), whereas 532 nm light excited primarily the donor.⁶ The dissociation of the exciplex, which forms under both 532 nm and 633 nm excitation,¹¹ contributed to the photocurrent in both cases. However, under 532 nm excitation, an order of magnitude higher photocurrent, as compared to that under 633 nm excitation, was observed due to strong contribution of charge carriers photogenerated in the ADT-TES-F host itself.

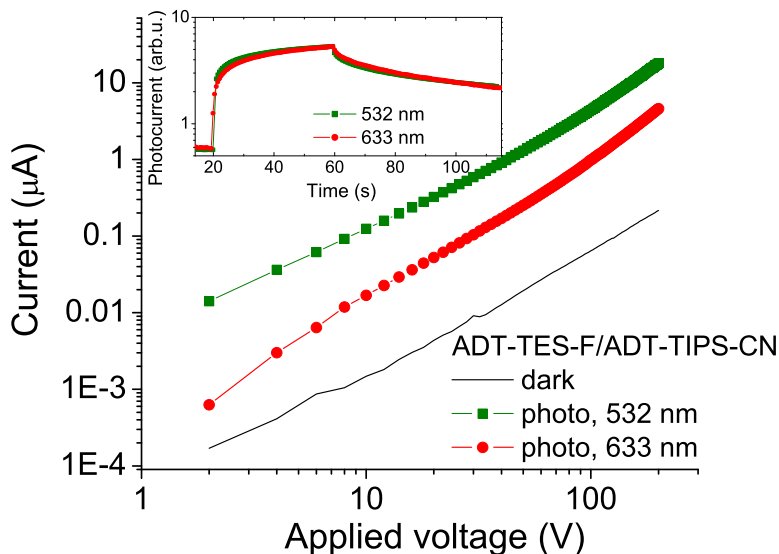


Figure 6. Photocurrent measured in the $S(3.6 \times 10^{-2}M)$ sample under 15 mW/cm^2 532 nm and 633 nm cw excitation. Dark current is also included. Inset shows dynamics of the photocurrent, normalized by corresponding values at 60 s, under the two wavelengths, with illumination being turned on at 20 s and off at 60 s.

The inset of Fig. 6 shows photocurrent dynamics under 15 mW/cm^2 cw illumination at 532 nm and 633 nm. At these wavelengths, the dynamics are similar, indicating that differences in charge carrier generation pathways between these two wavelengths do not have a large effect on charge carrier dynamics on the order of tens of seconds.

4. CONCLUSIONS

In summary, we explored the effect of solution deposition technique on aggregation processes and donor-acceptor interactions in functionalized ADT materials. While both drop casting and spin casting resulted in ADT aggregation, aggregates with different properties were obtained. In drop cast samples, red shifted PL spectra, which suggest larger aggregates, as compared to those in spin cast samples, were observed both in pristine ADT and in ADT/PMMA films. These differences in the PL properties were accompanied by differences in photoconductive

properties of drop and spin cast samples. In composite films of different ADT derivatives, ADT-TES-F (donor) and ADT-TIPS-CN (acceptor), the aggregation properties affected the onset of exciplex formation, which is a result of donor-acceptor interaction. This led to differences in the PL properties of drop and spin cast composite films.

Finally, we explored the dependence of photoconductivity on excitation wavelength in ADT-TES-F/ADT-TIPS-CN composites. We showed that although there is a significant increase in photoconductive response at 532 nm as compared to 633 nm, the charge carrier dynamics at time scales of seconds after photoexcitation are not affected.

5. ACKNOWLEDGEMENTS

This work was supported in part by the National Science Foundation via CAREER program (DMR-0748671) and Office of Naval Research (N00014-05-1-0019). W.E.B.S. thanks the SPIE Educational Scholarship in Optical Science and Engineering for support.

REFERENCES

1. S. R. Forrest, "The path to ubiquitous and low-cost organic electronic appliances on plastic," *Nature* **428**, p. 911, 2004.
2. H. Katz and J. Huang, "Thin-film organic electronic devices," *Annu. Rev. Mater. Res.* **39**, pp. 71–92, 2009.
3. J. E. Anthony, "Functionalized acenes and heteroacenes for organic electronics," *Chem. Rev.* **106**, pp. 5028–5048, 2006.
4. S. Subramanian, S. K. Park, S. R. Parkin, V. Podzorov, T. N. Jackson, and J. E. Anthony, "Chromophore fluorination enhances crystallization and stability of soluble anthradithiophene semiconductors," *J. Am. Chem. Soc.* **130**, p. 2706, 2008.
5. S. K. Park, D. A. Mourey, S. Subramanian, J. E. Anthony, and T. N. Jackson, "High-mobility spin-cast organic thin film transistors," *Appl. Phys. Lett.* **93**, p. 043301, 2008.
6. A. D. Platt, J. Day, S. Subramanian, J. E. Anthony, and O. Ostroverkhova, "Optical, fluorescent, and (photo)conductive properties of high-performance functionalized pentacene and anthradithiophene derivatives," *J. Phys. Chem. C* **113**(31), pp. 14006–14014, 2009.
7. J. Day, A. D. Platt, S. Subramanian, J. E. Anthony, and O. Ostroverkhova, "Influence of organic semiconductor-metal interfaces on the photoresponse of functionalized anthradithiophene thin films," *J. Appl. Phys.* **105**, p. 103703, 2009.
8. W. E. B. Shepherd, A. D. Platt, D. Hofer, O. Ostroverkhova, M. Loth, and J. E. Anthony, "Aggregate formation and its effect on (opto)electronic properties of guest-host organic semiconductors," *Appl. Phys. Lett.* **97**, p. 163303, 2010.
9. A. D. Platt, W. E. B. Shepherd, J. E. Anthony, and O. Ostroverkhova, "Photophysical and photoconductive properties of organic semiconductor composites," *SPIE Linear and Nonlinear Optics of Organic Materials IX* **7413**(1), p. 74130S, 2009.
10. J. Day, A. D. Platt, O. Ostroverkhova, S. Subramanian, and J. E. Anthony, "Organic semiconductor composites: influence of additives on the transient photocurrent," *Appl. Phys. Lett.* **94**, p. 013306, 2009.
11. W. E. B. Shepherd, A. D. Platt, M. J. Kendrick, M. A. Loth, J. E. Anthony, and O. Ostroverkhova, "Fret and exciplex formation in functionalized anthradithiophene derivatives and their impact on exciton and charge carrier dynamics in organic thin films," *Submitted*, 2010.
12. R. Al-Kaysi, T. Ahn, A. Müller, and C. Bardeen, "The photophysical properties of chromophores at high (100 nm and above) concentrations in polymers and as neat solids," *Phys. Chem. Chem. Phys.* **8**(29), pp. 3453–3459, 2006.
13. L. B. Schein, D. S. Weiss, and A. Tyutnev, "The charge carrier mobility's activation energies and pre-factor dependence on dopant concentration in molecularly doped polymers," *Chem. Phys.* **365**(3), pp. 101–108, 2009.

14. O. Ostroverkhova, S. Shcherbina, D. G. Cooke, R. F. Egerton, F. A. Hegmann, R. R. Tykwinski, S. R. Parkin, and J. E. Anthony, "Optical and transient photoconductive properties of pentacene and functionalized pentacene thin films: Dependence on film morphology," *J. Appl. Phys.* **98**, p. 033701, 2005.
15. B. Rand, J. Xue, S. Uchida, and S. Forrest, "Mixed donor-acceptor molecular heterojunctions for photovoltaic applications. 1. material properties," *J. Appl. Phys.* **98**, p. 124902, 2005.